BMB
reports

Cytosolic prion protein induces apoptosis in human neuronal cell SH-SY5Y via mitochondrial disruption pathway

Xin Wang[1,2], Chen-Fang Dong[1], Qi Shi[1], Song Shi[1], Gui-Rong Wang[1], Yan-Jun Lei[1,3], Kun Xu[1,3], Run An[1,3], Jian-Ming Chen[1], Hui-Ying Jiang[1], Chan Tian[1], Chen Gao[1], Yu-Jun Zhao[2], Jun Han[1] & Xiao-Ping Dong[1,]*

[1]State Key Laboratory for Infectious Disease Prevention and Control, National Institute for Viral Disease Control and Prevention, Chinese Center for Disease Control and Prevention, Ying-Xin Rd 100, Beijing 100052, [2]College of Animal Husbandry and Veterinary Medicine, Shenyang Agricultural University, Dongling Rd 120, Shenyang 110161, [3]School of Medicine, Xi'an Jiao-Tong University, Xi'an 710061, China

Different neurodegenerative disorders like prion disease, is caused by protein misfolding conformers. Reverse-transfected cytosolic prion protein (PrP) and PrP expressed in the cytosol have been shown to be neurotoxic. To investigate the possible mechanism of neurotoxicity due to accumulation of PrP in cytosol, a PrP mutant lacking the signal and GPI (CytoPrP) was introduced into the SH-SY5Y cell. MTT and trypan blue assays indicated that the viability of cells expressing CytoPrP was remarkably reduced after treatment of MG-132. Obvious apoptosis phenomena were detected in the cells accumulated with CytoPrP, including loss of mitochondrial transmembrane potential, increase of caspase-3 activity, more annexin V/PI-double positive-stained cells and reduced Bcl-2 level. Moreover, DNA fragmentation and TUNEL assays also revealed clear evidences of late apoptosis in the cells accumulated CytoPrP. These data suggest that the accumulation of CytoPrP in cytoplasm may trigger cell apoptosis, in which mitochondrial relative apoptosis pathway seems to play critical role. [BMB reports 2009; 42(7): 444-449]

INTRODUCTION

Prion diseases, or transmissible spongiform encephalopathies (TSE), are a group of neurodegenerative disorders that afflict humans and animals, including Creutzfeldt-Jakob disease (CJD) in human, scrapie in sheep and goat, and bovine spongiform encephalopathy (BSE) in cattle (1). The underlying cause of prion disease is the conversion of a host-derived cellular prion protein (PrP^{C}) to the infectious scrapie prion protein (PrP^{Sc}), a misfolded and proteinase K (PK)-resistant isoform (2). Propagation and accumulation of infectious prions have tightly linked to the pathogenesis of prion disease. However, transgenic mouse models have revealed that misfolding or mistargeting of PrP^{C} can also induce neuronal cell death in the absence of infectious prions (3). Mice expressing a PrP mutant with a deleted N-terminal and C-terminal signal acquired ataxia due to cerebellar degeneration and gliosis (4). Moreover, changes of the normal secreting and maturing pathway of wild-type (WT) PrP, especially the PrP mutants, such as Y145STOP and Q217R, in the presences of proteasome inhibitors, will cause obvious cytotoxic activity in the cultured cells, possibly due to the generation of intracellular PrP. In that case, the normally secreted PrP is subjected to the degradative pathway termed endoplasmic reticulum (ER) associated protein degradation (ERAD), possibly to eliminate misfolded PrP molecules (4). The presence of PrP in the cytosol (CytoPrP) suggests that deregulation of the proteasome system during aging may result in the accumulation of cytotoxic PrP molecules (5).

Although the cytotoxic effects of CytoPrP have been repeatedly observed in several cell lines (3), there is evidence that the expression of CytoPrP seems not to interfere with cell viability (6). Additionally, the mechanism of cell death after accumulation of CytoPrP is not fully described. In this study, two PrP recombinant proteins, the full-length human PrP (PrP1-253) and the truncated one with deletion of the N- and C-terminal peptides (PrP23-230) were introduced into human neuroblastoma cell line SH-SY5Y. In the presence of proteasome inhibitor, the truncated PrP23-230 was accumulated in cytoplasm. Remarkable cytotoxic effects significant apoptosis evidences were identified in the cells receiving CytoPrP after treatment of proteasome inhibitor.

RESULTS AND DISCUSSION

Accumulation of CytoPrP in the cells is controlled by the presence of proteasomal inhibitor MG-132

To achieve subcellular targeting of PrP to cytosol, an mammalian expressing plasmid expressing human PrP from aa 23 to 230 was generated, which lacked the authentic ER signal peptide (aa 1-22) and C-terminal GPI sequence (aa 231-253) (Fig. 1A). The recombinant plasmids expressing the full length human PrP (aa 1-253) and cytosol PrP (aa 23-230) were transiently transfected into SH-SY5Y cells for 24 hours. Western

*Corresponding author. Tel: 86-10-83534616; Fax: 86-10-63532053; E-mail: dongxp238@sina.com

Received 19 June 2008, Accepted 3 November 2008

Keywords: Apoptosis, CytoPrP, Cytotoxicity, Prion, Proteasome

blots revealed clear PrP signals in the cells expressing the PrP1-253, migrating at the position between *Mr* 25 and 35 KD (Fig. 1B, lane 2), whereas no positive signal in the cells receiving plasmid pcDNA-CytoPrP (lane 6). To address whether the absence of PrP signal in the cells transfected with pcDNA-CytoPrP was due to endogenous proteolysis, various amounts of proteasomal inhibitor MG-132 were added into the culture medium. A single 23 KD PrP-specific band was identified and the reactive intensity became stronger along with the increase of MG-132 (Fig 1B, lane 3-5), while the amounts of the expressed PrP1-253 did not change significantly (Fig 1B, lane 1 and 2). It suggests that inhibition of cellular proteolysis contributes to the accumulation of CytoPrP in cytoplasm.

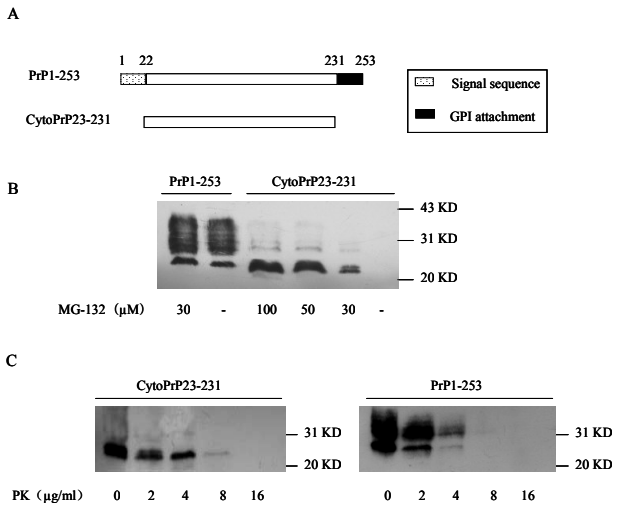

Fig. 1. Identification of expressions of CytoPrP and PrP1-253 in SH-SY5Y cells. (A) Schematic representation of human PrP1-253 and CytoPrP23- 230 constructs. The full length human PrP comprises 253 aa including N-terminal signal sequence (from aa 1 to 22) and C-terminal GPI sequence (from aa 231 to 253). CytoPrP is from aa 23 to 230. (B) Western blots of expressions of PrP1-253 and CytoPrP with PrP-specific mAb 3F4. Preparations of PrP1-253 and CytoPrP were shown above. Additions of MG-132 in the culture medium were illustrated below. (C) PK resistance. Total cell lysates were treated with various concentrations of PK at 37°C for 30 min before Western blot. Preparations of PrP1-253 or CytoPrP were shown above. PK concentrations were indicated below. Molecular size markers were indicated right.

To investigate whether the accumulated CytoPrP in cytoplasm has potential PK-resistance, various transfected cells were exposed to 30 μM MG-132 for 4 hours and cellular lysates were digested with PK. Western blots identified that the signals of the expressed PrP1-253 were detectable in the preparation treated with 4 μg/ml PK at final concentration, while CytoPrP were observed in the reaction of 8 μg/ml PK (Fig. 1C). It seems that the CytoPrP accumulated in cytoplasm possesses slightly stronger resistance to PK digestion.

The accumulation of CytoPrP causes cytotoxic effect to SH-SY5Y cells

To see the influence of accumulation of CytoPrP on the growth abilities of the cultured cells, the viabilities of transfected cells were measured with Trypan blue and MTT assays. MTT assays of the preparations 24 and 48 hours after transfection revealed that the cell viabilities of various groups were quite comparable (Fig. 2A). However, in the presence of MG-132, the viability of the cells expressing CytoPrP dropped remarkably, while viability of the cells expressed PrP1-253 remained unchanged compared with that without MG-132 as well as the cells transfected with plasmid pcDNA3.1 (Fig. 2A). Statistic analysis of the cell viabilities of CytoPrP before and after treatment of MG-132 showed

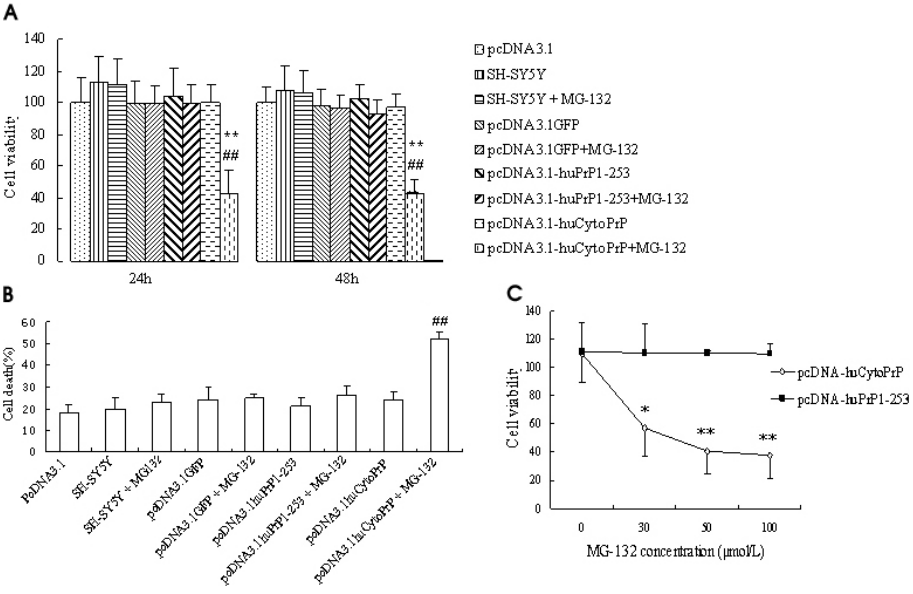

Fig. 2. Influences of the expressions of CytoPrP and PrP1-253 on the cell viability in the presences of MG-132 or not. (A) MTT assay 24 or 48 hours post-transfection. (B) Trypan blue staining 24 hours post-transfection. Statistical differences of the data of CytoPrP with MG-132 compared with that of PrP1-253 with MG-132, and with that of CytoPrP without MG-132 were illustrated as $^{*}P < 0.05$, $^{**}P < 0.01$, and $^{\#}P < 0.05$, $^{\#\#}P < 0.01$, respectively. (C) Dose-associated influences of MG-132. MTT assays for measuring cell viability after treatment of MG-132 for 4 hours. Statistical compared with the group of 0 μl MG-132 were illustrated as: $^{*}P < 0.05$, $^{**}P < 0.01$. The average data of each preparation was calculated based on three independent experiments and represented as mean ± S.D.

significantly difference ($P < 0.01$). Trypan blue assays also demonstrated the same phenomenon, that the death percentage (%) of cells transfected with pcDNA3.1-huCytoPrP after exposing to MG-132 was significantly lower than that without MG-132, as well as the others, showing significantly difference ($P < 0.01$, Fig. 2B). Furthermore, in the presences of 0, 30, 50, and 100 μM MG-132, the viabilities of cells expressing huPrP1-253 maintained unchanged, while that of the cells expressing CytoPrP reduced obviously, showing a dose-dependant manner (Fig. 2C).

CytoPrP induced the cytotoxic effect in SH-SY5Y cells is associated with apoptosis

To exclude the possible influence of MG-132 on the apoptosis event in the experimental condition, SH-SY5Y cells and the cells receiving pcDNA3.1 and pcDNA3.1-huPrP1-253 were exposed to 30 μM MG-132 for 4 hours and the cellular caspase-3 activities were assayed. No difference was found in each group regardless of presence or absence of MG-132 (data not shown). Cells transfected with PrP expressing plasmids before and after treatment of MG-132 were incubated with annexin V-FITC and PI and analyzed in flow cytometry. The percentages of the annexin V and annexin V/PI-double positive-stained cells in the groups receiving plasmid pcDNA3.1, pcDNA3.1-huPrP1-253 and pcDNA3.1-huCytoPrP before incubation of MG-132 were comparable, while that in the cells transfected with pcDNA3.1-huCytoPrP after treatment of MG-132 was remarkably increased (Fig. 3A). Calculating the rates of apoptosis cells revealed significantly statistic difference between the cells accumulated with CytoPrP and the others ($P < 0.01$, Fig. 3B).

The apoptosis phenomenon in the cells accumulated with CytoPrP was further confirmed via DNA fragmentation assays. Clearly DNA ladders in agarose electrophoresis gel were observed in the cells accumulated with CytoPrP, but not in the cells receiving plasmid pcDNA3.1, pcDNA3.1-huPrP1-253 and pcDNA3.1-huCytoPrP without incubation of MG-132 (Fig. 3C). To get further more evidences of apoptosis, SH-SY5Y cells accumulated with CytoPrP were tested by TUNEL. TUNEL-positive nuclei with condensing yellow-stained granule were frequently observed in the cells accumulated with CytoPrP after treatment of MG-132, but rarely observed in rest preparations. Evaluation of the respective apoptosis indexes (AI) identified a markedly increase in the accumulated with CytoPrP, revealing significantly statistic difference compared with the rest groups ($P < 0.01$, Fig. 3D).

Rapid intracellular apoptotic events in response to CytoPrP

Mitochondrial dysfunction characterized by a loss of transmembrane potential (Ψm) is a central event in many cases of apoptosis (7). Analyses of the changes of Ψm in the cells transfected with different PrP expressing plasmids demonstrated an extensive loss of Ψm in preparation of CytoPrP accumulation after incubated with MG-132 for 4 hours, while the cells ex-

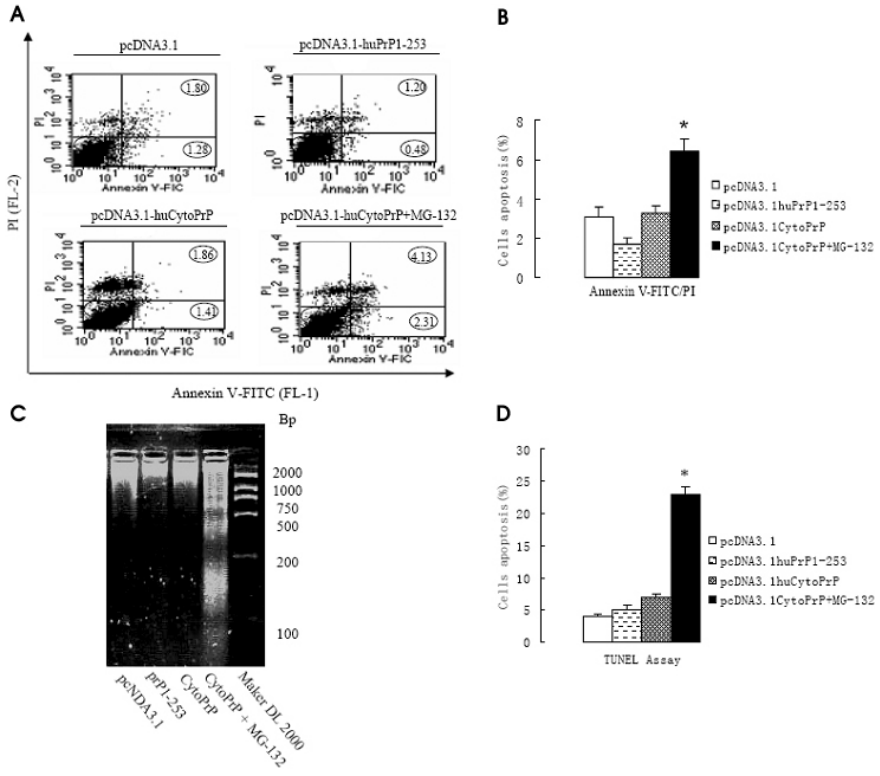

Fig. 3. Accumulation of CytoPrP induced apoptosis in SH-SY5Y cells. (A) Flow cytometry assays of annexin V/PI double staining. X axis indicated the numbers of Annexin V- FITC stained cells. Y axis indicated the numbers of PI strained cells. Annexin V-FITC positive stained cells were marked as FL-1 and PI-stained cells were marked as FL-2. The percentage of the overall population in each quadrant was given in circles. (B) Statistical graph of annexin V-FITC/PI staining. (C) Agarose electrophoresis of DNA ladder patterns. Lane 1, pcDNA3.1 control plasmid; lane 2, PrP1-253; lane 3, CytoPrP before incubation of MG-132; lane 4, CytoPrP after incubation of MG-132; lane 5, DNA marker DL 2000 (Takara). (D) TUNEL assays. SH-SY5Y cells were transfected with various plasmids of PrP for 24 hours. The index of cells apoptosis of each preparation was illustrated in Y axis. Apoptosis degree of each group was shown as apoptosis index evaluated by counting the percentage of apoptotic cells. The average data of each preparation were calculated based on three independent experiments. **indicated $P < 0.01$.

pressing CytoPrP without treatment of MG-132 showed the similar patterns as that receiving plasmid pcDNA3.1 (Fig. 4A). Measurements of the activities of caspase family found that the value of the activity of caspase-3 in the cells expressing CytoPrP after incubation with MG-132 for 4 hours was higher than that expressing CytoPrP without MG-132 and that expressing PrP1-253 after incubation with MG-132, showing significantly statistical difference ($P < 0.01$, Fig. 4B).

Accumulation of CytoPrP in cytoplasm leads to reduction of Bcl-2 levels

To address whether the possible changes of Bcl-2/Bax after accumulation of CytoPrP in cytoplasm, the levels of Bcl-2 and Bax in the cellular lysates prepared from the cells receiving plasmid pcDNA-huCytoPrP, pcDNA3.1 and pcDNA3.1-huPrP1-253 before and after incubation of MG-132 were comparatively evaluated by Western blots. It showed that the signals of Bcl-2 in the cells accumulated with CytoPrP were weaker than that of other preparations, while the signals of Bax did not vary largely among the groups (Fig. 4C). Analyses of the relative gray values of Bcl-2/Bax signals in each preparation after equilibrating with that of each internal actin signal revealed a significant reduction of Bcl-2 in the cells accumulated with CytoPrP ($P < 0.01$) (Fig. 4D).

In line with previous study (8), the ability of the cell growth starts to be hindered markedly after accumulation of immature PrP in cytoplasm. Apoptosis phenomena have been found not only in the brains of different human and animal TSEs *in vivo*, but also in the cell cultures expressing mutated PrPs *in vitro* (3, 8). Our previous studies have also identified that removal of glycosylation of PrP provokes apoptosis in the cultured cells (9). An important event in the above process is mitochondrial dysfunction. As a well known event in apoptosis, mitochondrial dysfunction is documented as loss of Ψm, leading to the opening of the permeability transition pore and release of solutes from the mitochondria (10). Caspase-3 can cleave many active proteins related with cell life-cycle, including Bcl-2. Bcl-2 is an essential anti-apoptosis protein which is capable of inhibiting apoptosis induced by a wide variety of apoptotic stimuli (11). Similar changes of Bcl-2/Bax have been detected in the other study when inducing recombinant PrP mutants into cells (9). PrP106-126 fragment is able to reduce the level of Bcl-2 mRNA in neuron cells *in vitro* experiments (12). These data strongly highlight the critical role of mitochondrial relative apoptosis pathway in the cell death program due to introduction of mutated PrPs and alternation of normal maturing process of PrP.

PrP^C is a cellular membrane protein that begins its journey to the cell surface in ER. Like many proteins that traffic through the ER (13), a substantial fraction of misfolded PrP is normally generated and transported to the cytosol and degraded by pro-

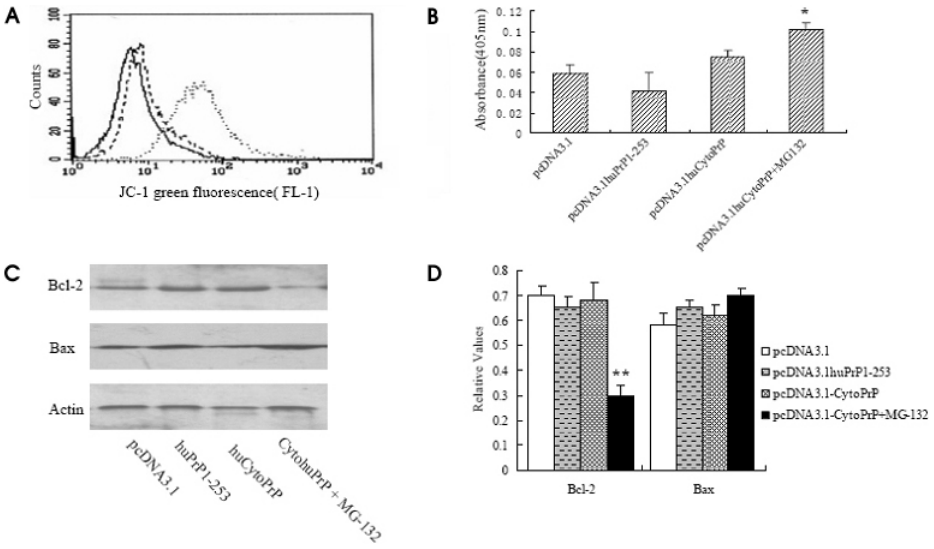

Fig. 4. Changes of mitochondrial depolarization, caspase activation and Bcl-2 in the cells accumulated by CytoPrP. (A) Measurement of extensive depolarization of the mitochondrial membrane represented by an increase in FL-1 24 hours after transfection using JC-1 as fluorescent probe. Black line represented the cells transfected with pcDNA3.1. Short-bar line was the cells transfected with pcDNA3.1-huCytoPrP before incubation of MG-132 and dot line was the cells transfected with pcDNA3.1-huCytoPrP after incubation of MG-132. X-axis indicateed the quantities of JC-1 green fluorescence (FL-1). (B) Measurement of caspase-3 activity. The average data of each preparation were calculated based on three independent experiments and represented as mean ± S.D. "*" represented statistic difference ($P < 0.05$). (C) Western blots of Bcl-2 and Bax protein. Cell lysates were prepared 24 hours after transfection and protein concentrations in each preparation are equilibrated before SDS-PAGE. The expressions of β-actin were used as internal control. Lane 1, pcDNA3.1; lane 2, PrP1-253; lane 3, CytoPrP before incubation of MG-132; lane 4, CytoPrP after incubation of MG-132. (D) Quantitative analyses of the Bcl-2 and Bax immunoblots in each preparation. The average gray value of Bcl-2 or Bax was obtained from three independent tests. Relative gray value of Bcl-2 or Bax in each preparation was obtained by dividing the gray values of each reaction by that of actin. The average data of each preparation were calculated based on three independent experiments. ** indicated $P < 0.01$.

teasomes (4). Generally, PrP in cytosol is degraded so rapidly that it is usually undetectable. However, when the cellular endogenous proteasome's activity is hindered, the CytoPrP may accumulate. Recent data shows that the signal sequence of PrP is insufficient for complete protein translocation into the ER, giving rise to a nontranslocated PrP fraction in cytosol (14), such as the pathogenic mutants W160Stop and W145Stop that are partially mislocated in cytosol (15). Alternatively, access to the cytosol is possible via retrograde translocation of PrP out of the ER; this route has been demonstrated for WT PrP and another pathogenic PrP mutant, D177N (4). In line with other studies, our data confirm again that the CytoPrP presented in cytoplasm after proteasomal impairment shows some PK-resistant characteristics. Therefore, it is possible that the efficiency of the ubiquitin-proteasomal system will decrease along with aging, leading the aged neurons more vulnerable to the accumulation of misfolded proteins. However, some studies have also revealed that accumulation of PrP in cytosol is not toxic for neurocytes and the CytoPrP is inaccessible to PrP^{Sc} in transgenic mice (6, 16), which may indicate a more complicated mechanism. Further analysis of the cellular proteasomal status during TSE will help to address the role of proteasomal impairment in the pathogenesis of TSE.

MATERIALS AND METHODS

Plasmid construction

Human PrP gene encoding the peptide from residues 23 to 230 (PrP23-230) was amplified with a PCR technique, using recombinant plasmid pT-huPrP23-230 as template (17), with forward primer (5′-ggatccatgaagaagcgcccgaagcctggag-3′, with BamHI site underlined) and reverse primer (5′-gcggccgctcacatgctcgatcctct ctggtaatag-3′, with Not I site underlined). After verified with sequencing analysis, the PCR product was cloned into vector pcDNA3.1, generating plasmid pcDNA3.1-huCytoPrP. The recombinant plasmid pcDNA3.1-PrP1-253 containing full-length WT human *PRNP* segment encoding aa 1-253 was generated previously (9). To construct plasmid containing full-length enhanced green fluorescent protein (EGFP), the sequence of EGFP was amplified from commercially recombinant plasmid pEGFP-N1 (Clontech) by PCR, using forward primer (5′-ggatccatggtgagcaagggcga-3′, with BamHI site underlined) and reverse primer (5′-gcggccgcttacttgtacagctcgtccat-3′, with Not I site underlined). The PCR product was cloned into pcDNA3.1, generating plasmid pcDNA3.1-GFP.

Cell culture, transfection, proteasomal inhibition, and proteinase K digestion

SH-SY5Y cells were maintained in DMEM (Gibco BRL). and plated into 6-well or 96-well plates (Falcon) 24 hours before transfection. Different amounts of plasmids (2 μg DNA per well in 6-well plate and 0.2 μg in 96-well plate) were transfected into the cells with Lipofectamine^{TM} 2000 transfection reagent (Invitrogen, USA). Cells were harvested by trypsin/EDTA in PBS 24 or 48 hours after transfection. To see the influence of proteasomal inhibitor, different concentrations of MG-132 (Calbiochem) dissolved in dimethyl sulfoxide (DMSO) were supplied into the culture medium at 37°C for 4 hours. For proteolysis experiments, cellular lyses were incubated with PK at various concentrations at 4°C for 30 min. The reaction was terminated by adding Pefabloc SC (Roche).

Western blots

The cellular lysates were separated by 15% SDS-PAGE and electro-transferred onto nitrocellulose membranes described previously (18). After blocking with 5% deffated milk in PBST (PBS, pH 7.6, containing 0.05% Tween-20), the membranes were incubated with 1:4000 PrP specific monoclonal antibody (mAb) 3F4 (Deko), or with 1 : 1,000 mouse mAbs anti-human Bcl-2 and 1 : 2,000 anti-human Bax (Santa Cruz), or 1 : 1,000 mAb anti-human β-actin (Santa Cruz) at room temperature for 2 hours, and subsequently with 1 : 4,000 horseradish peroxidase (HRP)-conjugated anti-mouse IgG (Santa Cruz). The reactive signals were visualized by ECL kit (PE Applied Biosystems).

Trypan blue and MTT assays

Cells were cultured in 96-well plates. 24 hours after transfection, and harvested and stained with the DNA-binding dye trypan blue (Sigma) for 30 min. The numbers of trypan blue-positive stained cells were counted under microscope. MTT assays were performed by addition of 3-(4, 5-Dimethylthiazol-2-yl)-2, 5-diphenyl-2H-tetrazolium bromide (MTT, Sigma) to the culture medium at final concentration of 5 mg/ml at 37°C for 4 hours, 24 and 48 hours after transfection. The reaction was terminated by removal of the supernatant and addition of 200 μl DMSO to dissolve the formazan product. The plates were read at 540 nm on a microELISA plate reader (Thermo MK3). Each assay was performed in duplication of at least four wells.

DNA fragmentation assay

DNA fragmentation in the transfected cells was determined by the DNA-laddering technique. Briefly, cells were lysed in the buffer containing 5 mM Tris-HCl, pH7.5, 20 mM EDTA and 0.2% Triton-X 100 at 4°C for 30 min. After centrifuging, the supernatants were treated with 0.3 mg/ml PK at 60°C for 30 min, extracted in phenol/chloroform and in chloroform/isoamylalcohol (24:1), and subsequently precipitated in 100% ethanol. The pellets were washed in 70% ethanol and resuspended in 25 μl of Tris/EDTA buffer (pH 7.5). 10 μl of each preparation were subjected to 2.0% agarose gel electrophoresis and stained with ethidium bromide.

Annexin V-FITC binding

Binding of annexin V-FITC and uptake of propidium iodide (PI) (Trevigen, Minneapolis) of the cells were assessed by a FACScan flow cytometry (Becton Dickinson). Briefly, 24 hours after transfection, cells were harvested, resuspended and incubated with annexinV-FITC (1×) and PI (5 μg/ml) in the dark at room temper-

ature for 15 min. Fluorescence was measured through a 530/30 band filter (FL-1) to monitor annexin V-FITC binding and through a 585/42 band filter (FL-2) to monitor PI uptake.

Measurement mitochondrial membrane potential (Ψm)

Cells were harvested and treated with the final concentration of 2 μM JC-1 (Molecular Probes, Netherlands) at 37°C for 30 min. Ψm was measured by fluorescence emission on a FAC Scan flow cytometry (Becton Dickinson). Fluorescence emission was collected through FL-1 on a log scale.

Caspase-3 activity

Caspase-3 activity was measured following the manufacture's instruction (Sigma). Briefly, Ac-DEVE-pNA (Sigma) was used as the substrate for activated caspase-3, and 1-2 $\times$ 10^6 cells were typically used. Reactions were conducted in 96 well plates at 37°C for 2 hours in the dark. Absorbance was determined with a microELISA plate reader (Thermo MK3) at 405 nm.

TUNEL assay

Potential DNA fragment was examined by the TUNEL apoptosis detection kit (Chemicon, USA). Briefly, 24 hours after transfection, the cells were fixed with 4% paraformaldehyde in 0.1 M NaH_2PO_4, pH 7.4, and endogenous peroxidase was inactivated by 3% H_2O_2. Cells were incubated with a solution containing biotin-dUTP and the terminal deoxynucleotidyl transferase (TdT) for 60 min. After end-horseradish peroxidase, stained with diaminobenzidine, and counterstained with ethyl green to detect biotin-labeled nuclei. Apoptosis bodies were stained as brown. Cell nuclei were counted under the light microscope. Apoptosis index (AI) was calculated as the percentage of apoptosis cells. At least three independent observers counted the positive-staining nuclei in three fields.

Statistic analysis

Quantitative analysis of immunoblot images was carried out using computer-assisted software Image Total Tech (Pharmacia). Briefly, the image of immunoblot was scanned with Typhoon (Pharmacia) and digitalized, saved as TIF format. The values of each target blot were evaluated. All data are presented as the mean $\pm$ SD. Statistical analysis was performed using the *T* test. Probabilities of less than 0.05 were considered to be statistically significant.

Acknowledgement

This work was supported by National Science and Technology Task Force Project (2006BAD06A13-2), National Basic Research Program of China (973 Program) (2007CB310505) and Chinese National Natural Science Foundation Grants 30571672, 30500018, 30771914 and 30800975.

REFERENCES

1. Prusiner, S. B. (1998) Prions. *Proc. Natl. Acad. Sci. U.S.A.* **95**, 13363-13383.
2. Aguzzi, A. and Polymenidou, M. (2004) Mammalian prion biology: one century of evolving concepts. *Cell* **116**, 313-327.
3. Ma, J., Wollmann, R. and Lindquist, S. (2002) Neurotoxicity and neurodegeneration when PrP accumulates in the cytosol. *Science* **298**, 1781-1785.
4. Ma, J. and Lindquist, S. (2001) Wild-type PrP and a mutant associated with prion disease are subject to retrograde transport and proteasome degradation. *Proc. Natl. Acad. Sci. U.S.A.* **98**, 14955-14960.
5. Keller, J. N., Gee, J. and Ding, Q. (2002) The proteasome in brain aging. *Ageing Res. Rev.* **1**, 279-293.
6. Fioriti, L., Dossena, S., Stewart, L. R., Stewart, R. S., Harris, D. A., Forloni, G. and Chiesa, R. (2005) Cytosolic prion protein is not toxic in N2a cells and primary neurons expressing pathogenic PrP mutations. *J. Biol. Chem.* **280**, 11320-11328.
7. Carmody, R. J. and Cotter, T. G. (2001) Signaling apoptosis: a radical approach. *Redox Report* **6**, 77.
8. Rambold, A. S., Miesbauer, M., Rapaport, D., Barke, T., Baier, M., Winklhofer, K. F. and Tatzelt, J. (2006) Association of bcl-2 with misfolded prion protein is linked to the toxic potential of cytosolic PrP. *Mol. Biol. Cell* **17**, 3356-3368.
9. Chen, L., Yang, Y., Han, J., Zhang, B. Y., Zhao, L., Nie, K., Wang, X. F., Li, F., Gao, C., Dong, X. P. and Xu C. M. (2007) Removal of the glycosylation of prion protein provokes apoptosis in SF126. *J. Biochem. Mol. Biol.* **41**, 662-669.
10. Seo, Y. W., Park, S. Y., Yun, C. W. and Kim, T. H. (2006) Differential efflux of mitochondrial endonuclease G by hNoxa and tBid. *J. Biochem. Mol. Biol.* **39**, 556-559.
11. Adams, J. M. and Cory, S. (1998) The Bcl-2 protein family: Arbiters of cell survival. *Science* **281**, 1322-1326.
12. Perovic, S., Schroder, H. C. and Pergande, G. (1997) Effect of flupirtine on bcl-2 and glutathione level in neuronal cells treated *in vitro* with the prion protein fragment (PrP106-126). *Exp. Neurol.* **147**, 518-524.
13. Kopito, R. R. (1997) ER quality control: the cytoplasmic connection. *Cell* **88**, 427-430.
14. Rane, N. S., Yonkovich, J. L. and Hedge, R. S. (2004) Protection from cytosolic prion protein toxicity by modulation of protein translocation. *EMBO J.* **23**, 4550-4559.
15. Zanusso, G., Petersen, R. B. and Jin, T. (1999) Proteasomal degradation and N-terminal protease resistance of the codon 145 mutant prion protein. *J. Biol. Chem.* **274**, 23396-23404.
16. Norstrom, E. M., Ciaccio, M. F., Rassbach, B., Wollmann, R. and Mastrianni, J. A. (2007) Cytosolic prion protein toxicity is independent of cellular prion protein expression and prion propagation. *J. Virol.* **81**, 2831-2837.
17. Dong, C. F., Wang, X. F., Wang, X., Shi, S., Wang, G. R., Shan, B., An, R., Li, X. L., Zhang, B. Y., Han, J. and Dong, X. P. (2008) Molecular interaction between prion protein and GFAP both in native and recombinant forms *in vitro*. *Med. Microbiol. Immunol.* **197**, 361-368.
18. Dong, C. F., Shi, S., Wang, X. F., An, R., Li, P., Chen, J. M., Wang, X., Wang, G. R., Shan, B., Zhang, B. Y., Han, J., and Dong, X. P. (2008) The N-terminus of PrP is responsible for interacting with tubulin and fCJD related PrP mutants possess stronger inhibitive effect on microtubule assembly *in vitro*. *Arch. Biochem. Biophys.* **480**, 83-92.